Optics Letters

Deep-learning-assisted sidewall profiling white light interferometry system for accurately measuring 3D profiles and surface roughness on the groove sidewalls of precision components

Xiangyu Zhao,[1] Jinsong Zhang,[1] Renlong Zhu,[2] Yijun Xie,[2] Zhengqiong Dong,[2] Lei Nie,[2] Shiyuan Liu,[1,3,5] and Jinlong Zhu[1,3,4,*]

[1]State Key Laboratory of Intelligent Manufacturing Equipment and Technology, Huazhong University of Science and Technology, Wuhan 430074, China
[2]Hubei Key Laboratory of Manufacture Quality Engineering, Hubei University of Technology, Wuhan 430068, China
[3]Optics Valley Laboratory, Wuhan, Hubei 430074, China
[4]Research Institute of Huazhong University of Science and Technology Shenzhen, Shenzhen 518057, China
[5]shyliu@hust.edu.cn
*jinlongzhu03@hust.edu.cn

Received 30 May 2024; revised 25 July 2024; accepted 28 July 2024; posted 30 July 2024; published 12 August 2024

The accurate measurement of surface three-dimensional (3D) profile and roughness on the groove sidewalls of components is of great significance to diverse fields such as precision manufacturing, machining processes, energy transportation, medical equipment, and semiconductor industry. However, conventional optical measurement methods struggle to measure surface profiles on the sidewall of a small groove. Here, we present a deep-learning-assisted sidewall profiling white light interferometry system, which consists of a microprism-based interferometer, an optical path compensation device, and a convolutional neural network (CNN), for the accurate measurement of surface 3D profile and roughness on the sidewall of a small groove. We have demonstrated that the sidewall profiling white light interferometry system can achieve a measurement accuracy of 2.64 nm for the 3D profile on a groove sidewall. Moreover, we have demonstrated that the CNN-based single-image super-resolution (SISR) technique could improve the measurement accuracy of surface roughness by over 30%. Our system can be utilized in cases where the width of the groove is only 1 mm and beyond, limited only by the size of the microprism and the working distance of the objective used in our system. © 2024 Optica Publishing Group. All rights, including for text and data mining (TDM), Artificial Intelligence (AI) training, and similar technologies, are reserved.

https://doi.org/10.1364/OL.531552

Components with grooves, such as valves, bearings, molds, pipelines, printed circuit boards, and surgical instruments, are widely used in various fields including aerospace [1], precision manufacturing and measurement [2,3], machining process research [4], energy transportation [5], photoelectronic industry [6,7], and medical equipment [8]. The 3D profiles of a component's groove sidewalls can affect the quality of assembly, resulting in issues such as incomplete sealing, increased friction and vibration, and accelerated wear [9–11]. In addition, the roughness of the groove sidewalls can impact the strength, fatigue properties, and working accuracy of the component [12–14]. Therefore, it is critical to accurately measure the 3D profiles and surface roughness on the groove sidewalls of precision components. Conventional measurement methods, such as white light interferometry (WLI) [15,16], diffraction phase microscopy (DPM) [17], fiber endoscope [18], laser confocal techniques [19,20], scanning electron microscopy (SEM) [21,22], atomic force microscopy (AFM) [23], and scanning probe microscopy (SPM) [24], have been demonstrated as powerful tools for 3D surface metrology. These techniques have the capability to measure the surface profile of a groove's sidewall by rotating the sample to a level such that the sidewall is perpendicular to the probe (i.e., a light beam, an electron beam, or an AFM cantilever). However, they cannot deal with scenarios where the depth-to-width ratio of the sample's groove is large by simply rotating the sample, due to the fact that the rotated sample may block the probe. Therefore, it is crucial to develop a method that can non-destructively measure the 3D profile and surface roughness on the groove sidewalls with a large depth-to-width ratio.

In this paper, we developed a deep-learning-assisted sidewall profiling white light interferometry (SPWLI) system, which combines an inserted microprism, a white light interferometry system (WLIS), and a convolutional neural network (CNN), to precisely reconstruct the 3D profile and surface roughness on the sidewall of a groove. The microprism, which is connected to the objective of a WLIS through rigid coupling, acts as the probe of our SPWLI system and is inserted into the groove to bend the beam for sidewall measurement. As a result, we can only choose an objective with a low numerical aperture (NA) in order to guarantee a long working distance for the endoscope. However, the low-NA objective reduces the resolution of the endoscope. Hence, we propose a CNN-based SPWLI (CNN-SPWLI), which

0146-9592/24/164634-04 Journal © 2024 Optica Publishing Group

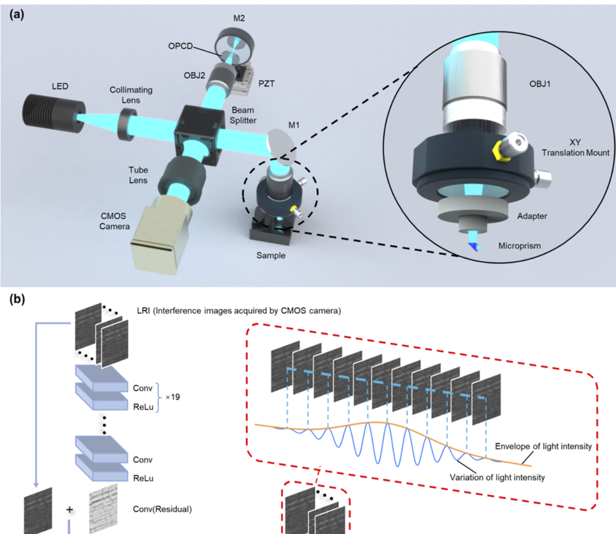

Fig. 1. Schematic diagram of the proposed SPWLI and the principle of the CNN-based resolution enhancement method. (a) Schematic diagram of the endoscope. The zoomed-in exploded drawing on the right shows how the microprism is connected to the measurement system. (b) Schematic network structure of the CNN-based resolution enhancement method for interferometric images. We cascade a pair of layers [convolutional (Conv) and rectified linear units (ReLu)] by 19 times. The initial low-resolution image (LRI) captured by the endoscope is cascaded through the layers and converted to a high-resolution image (HRI). The CNN predicts the residual image, and the LRI and residual image are summed to obtain the HRI.

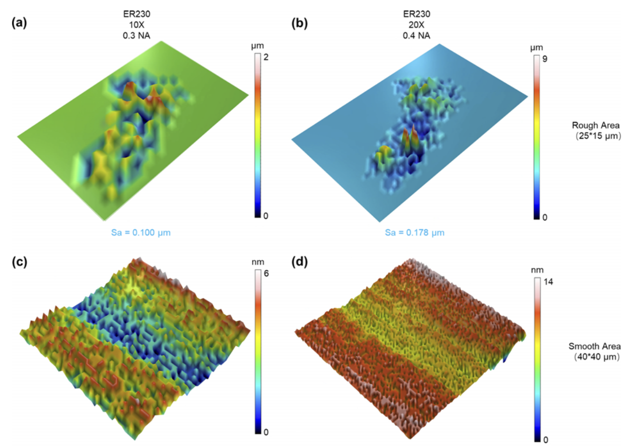

Fig. 2. Surface roughness in rough and smooth areas measured by a commercial WLI using objectives with different NA. The measurement results of rough areas using ER230 with (a) a 0.3-NA objective and (b) a 0.4-NA objective, respectively. Measurement results of smooth areas using ER230 with (c) a 0.3-NA objective and (d) a 0.4-NA objective, respectively. The size of the rough area shown in (a) and (b) is 25 µm long by 15 µm wide. The size of the smooth area shown in (c) and (d) is 40 µm long by 15 µm wide.

uses a residual learning method for the CNN to construct the mapping between the captured low-resolution interferometric images and the theoretical high-resolution interferometric images. Our experimental results demonstrated that the CNN-SPWLI can increase the measurement accuracy of surface roughness by over 30% when compared with that without using CNN. For small-diameter grooves, our method can measure depth-to-width ratios that are about six times greater than conventional WLI, and for large-diameter grooves, our method can be used without any limitations on depth-to-width ratios, which is not achievable with conventional WLI.

The proposed SPWLI is schematically shown in Fig. 1(a). We used an LED with a center wavelength of 455 nm and a bandwidth of 18 nm as the light source (model M455L4; Thorlabs Inc.). The light source is collimated by a collimating lens before entering a beam splitter. One beam goes toward the objective OBJ1 before entering the microprism, which is utilized to bend the beam for vertically illuminating the sidewall. The edge length of the microprism determines how small a groove we can measure. In this paper, we choose a microprism with an edge length of 0.5 mm, thus allowing us to measure the sidewall profile of a groove whose width can be as small as 1 mm. The reflected beam from the sidewall is captured by the same microprism and objective before entering the tube lens and the complementary metal–oxide–semiconductor (CMOS) camera. The other beam passes through the reference path, which consists of the objective OBJ2 and the high-quality reference mirror M2, before being captured by the same CMOS camera. By controlling a piezoelectric transducer (PZT) stage to drive the displacement of the reference mirror M2, the optical path difference between the two beams can be adjusted to produce interferograms in the CMOS camera.

The zoomed-in drawing on the right side of Fig. 1(a) shows how the microprism is connected to the measurement system. An in-house fabricated center-through-hole adapter is fixed inside the XY translation mount by a retaining ring, and the microprism is fixed on the adapter by the UV curing adhesive. By adjusting the displacement of the XY translation mount, the microprism can be aligned with the measurement system. In order to reduce the initial optical path difference between the two optical paths in the measurement system, we use two identical objectives in the system. Moreover, an optical path compensation device (OPCD) [i.e., an additional thin-film glass window; see Fig. 1(a)] was introduced to compensate for the additional optical path induced by the microprism. The refractive index of the microprism is n, thus the additional optical path difference introduced by the microprism is $d(n-1)$. Therefore, the thickness of the OPCD needs to be equal to the edge length of the microprism, and the OPCD needs to be made of the same material as the microprism. The conventional five-step phase shift algorithm [15] is used to process the interferogram images to obtain the surface 3D profiles.

In general, the measurement accuracy for the surface roughness of components is dominated by the NA of the objective of a measurement system, i.e., the resolution of the measurement system [25]. Figure 2 shows the 3D profiles and roughness on the surface of a component measured by a commercial WLI (model ER230; Atometrics, Inc.) with a 0.3-NA objective and a 0.4-NA objective, respectively. Here we use average surface roughness (Sa) to quantify the level of roughness in the measurement area. The average surface roughness (Sa) is defined as follows:

$$Sa = \frac{1}{N}\sum_{k=1}^{N}|z_k|, \tag{1}$$

where N is the total number of pixels in the measurement area and z_k is the height value of the k-th pixel. As shown

in Fig. 2, the measured average surface roughness (Sa) for the rough area on the component surface using the 0.3-NA objective and 0.4-NA objective were 0.1 µm and 0.178 µm, respectively. However, the measured Sa for the smooth area on the component using the 0.3-NA objective and 0.4-NA objective were 0.935 nm and 1.037 nm, respectively. The aforementioned experiments demonstrated that the measurement accuracy of surface roughness becomes worse if the area under measurement becomes rougher for a given low-NA objective. In order to enhance the measurement accuracy of surface roughness using a low-NA objective, the CNN [26] is utilized for performing SISR processing on the interferometric images. The network structure of CNN-based SISR processing for interferometric images is shown in Fig. 1(b), in which the first layer of the CNN network structure is the image input layer, followed by 19 pairs of cascaded convolutional (Conv) and rectified liner unit (ReLu) layers. The Conv layer consists of 64 filters with the size of $3 \times 3 \times 64$. Each filter operates on a 3×3 spatial region in 64 channels. The last layer consists of a filter with the size of $3 \times 3 \times 64$ for image reconstruction. In order to solve the problem that the size of the feature map decreases with each convolution operation, a zero-complement operation is needed before the convolution operation to keep all feature maps of the same size [27]. The network plays the role of adding more image details from the high-resolution interferometric images to the low-resolution interferometric images through network training. In order to implement the CNN-based SISR processing method, a large dataset including various interferometric images of groove sidewalls is required to train and validate the network. The training dataset was obtained by the commercial ER230 system with a high-NA objective and a low-NA objective. The closer the predicted residuals are to the actual residuals, the better the performance of the CNN. In order to accelerate the computation speed of the training process, we use the method of stochastic gradient descent with momentum to minimize loss function [28]. Here we use the loss function and network parameters from traditional CNNs for network training.

The SPWLI, the CNN-SPWLI, and the commercial WLI (ER230) were used to respectively measure the surface roughness on the sidewall of a machined component with a 1-mm groove width. The surface roughness on the groove sidewall of the component was firstly measured by the SPWLI with a 0.15-NA objective, after which the CNN-based SISR processing was applied to enhance the measurement results from the SPWLI. In order to evaluate the measurement accuracy obtained by the SPWLI and CNN-SPWLI, we cut the component along the centerline of the groove followed by using the commercial WLI ER230 (equipped with a 0.4-NA objective) to measure the same surface area. As a result, the measured value by the ER230 is treated as the golden standard for the comparison. As shown in Fig. 3, the measured Sa of two different areas on the sidewall using the CNN-SPWLI are 0.164 µm [Fig. 3(b)] and 0.138 µm [Fig. 3(e)], which are both closer to the golden standard [see Figs. 3(c) and 3(f)] when compared to the ones measured by the SPWLI [see Figs. 3(a) and 3(d)]. Therefore, the trained CNN could improve the measurement accuracy of surface roughness on the groove sidewall by at least 30% (the measured results of a groove with a large depth-to-width ratios are shown in Supplement 1).

We further evaluated the performance of the CNN-SPWLI by measuring the 3D profile and average roughness (Ra) of an in-house fabricated step sample, which is an etched triangle

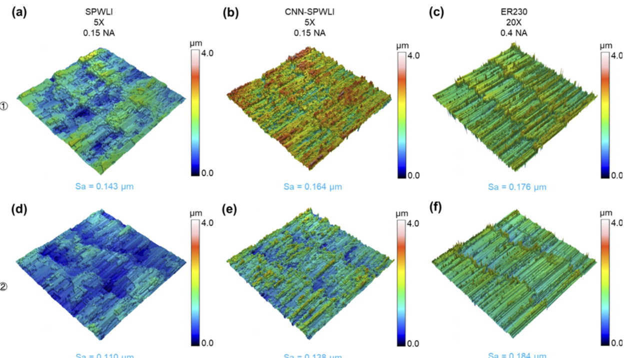

Fig. 3. Measurement results of surface roughness on the groove sidewalls. The measurement results of surface roughness using (a) the SPWLI with a 0.15-NA objective, (b) the CNN-SPWLI with a 0.15-NA objective, and (c) the ER230 with a 0.4-NA objective, respectively. (d)–(f) Measurement results of another area on the groove sidewall using the measurement methods in (a), (b), and (c), respectively. The two measurement areas are both 100 µm wide by 100 µm long.

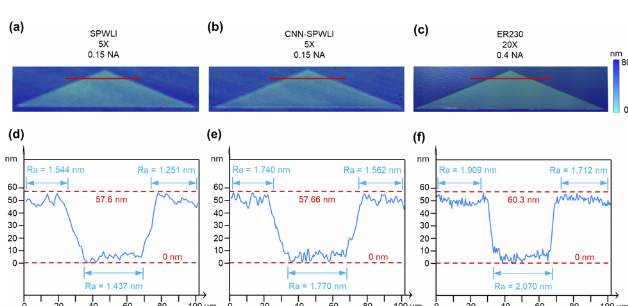

Fig. 4. Measurement results of 3D profiles and surface roughness on the groove sidewalls. The measurement results of 3D profiles and surface roughness using (a) the SPWLI with a 0.15-NA objective, (b) the CNN-SPWLI with a 0.15-NA objective, and (c) the ER230 with a 0.4-NA objective, respectively. (d), (e), and (f) Corresponding cross sections along the red lines in (a), (b), and (c). The three Ra measurement areas in (d), (e), and (f) correspond to the same horizontal axis, which are determined by the number of pixels in the image.

using electron-beam lithography (EBL) and inductively coupled plasma (ICP). We rotated the sample by 90° in order to mimic the scenario of a groove sidewall. The 3D profile and surface roughness on the groove sidewall were firstly measured by the SPWLI with a 0.15-NA objective, after which the CNN-based SISR processing was applied to enhance the measurement results from the SPWLI. Here we use the measurement results from the ER230 with a 0.4-NA objective as the golden standard for the comparison. The measurement results of 3D profiles using the SPWLI, CNN-SPWLI, and ER230 are shown in Figs. 4(a), 4(b), and 4(c), respectively. The reconstructed 3D profile by the SPWLI is less accurate than that measured by the ER230, because of the low-NA objective used in the SPWLI. The reconstructed 3D profile by the CNN-SPWLI recovers more details than that measured by the SPWLI. As shown in Fig. 4, the measured Ra of three areas along the cross sections using the CNN-SPWLI are 1.740 nm, 1.770 nm, and 1.562 nm [Fig. 4(e)], which are all closer to the golden standard [see Fig. 4(f)] when compared to the ones measured by the SPWLI [see Fig. 4(d)]. To be more

specific, the accuracies of Ra reconstructed by the CNN-SPWLI are improved by 53.70%, 52.61%, and 67.46%, respectively. The step heights measured by the CNN-SPWLI and ER230 are 57.66 nm and 60.3 nm respectively, with a difference of 2.64 nm, which demonstrates that the CNN-SPWLI is capable of achieving accurate measurements (nanometer accuracy) even with a low-NA objective.

This study presents a deep-learning-assisted sidewall profiling white light interferometry (SPWLI) system, which consists of a microprism-based interferometer, an optical path compensation device, and a CNN, for the accurate measurement of surface 3D profile and roughness on the sidewall of a small groove with nanometer accuracy. We have experimentally demonstrated that SPWLI can achieve a 2.64 nm measurement accuracy for 3D profile measurements, even using a low-NA objective. Moreover, we have demonstrated that the CNN-based SISR technique could improve the measurement accuracy of surface roughness by over 30%. We anticipate that this work could have a wide range of applications in fields such as aerospace, precision manufacturing, machining process research, energy transportation, photoelectronic industry, and medical equipment.

Funding. National Natural Science Foundation of China (52175509); National Key Research and Development Program of China (2023YFF1500900); Shenzhen Fundamental Research Program (JCYJ20220818100412027); Guangdong-Hong Kong Technology Cooperation Funding Scheme Category C Platform (SGDX20230116093543005); Innovation Project of Optics Valley Laboratory (OVL2023PY003).

Disclosures. The authors claim a C.N. patent and a U.S. patent on the presented method in this work through Huazhong University of Science and Technology.

Data availability. Data underlying the results presented in this paper are not publicly available at this time but may be obtained from the authors upon reasonable request.

Supplemental document. See Supplement 1 for supporting content.

REFERENCES

1. Y. Gong and E. J. Seibel, Opt. Eng. **56**, 014108 (2017).
2. J. Guo, D. Zhai, W. Lu, *et al.*, Opt. Laser Technol. **152**, 108133 (2022).
3. J. Zhu, J. Liu, T. Xu, *et al.*, Int. J. Extrem. Manuf. **4**, 032001 (2022).
4. A. Bhaskar, J. Philippe, F. Braud, *et al.*, Opt. Laser Technol. **138**, 106866 (2021).
5. C. Chen, C. Li, G. Reniers, *et al.*, J. Cleaner Prod. **279**, 123583 (2021).
6. J. LaDou, Int. J. Hyg. Environ. Health **209**, 211 (2006).
7. W. Chen, S. Liu, and J. Zhu, Int. J. Extrem. Manuf. **6**, 035501 (2024).
8. C. Culmone, G. Smit, and P. Breedveld, Addit. Manuf. **27**, 461 (2019).
9. Y. Wang, Y. Wang, L. Zheng, *et al.*, Sensors **22**, 1991 (2022).
10. M. Priest and C. M. Taylor, Wear **241**, 193 (2000).
11. T. Yang, T. Liu, W. Liao, *et al.*, J. Mater. Process. Technol. **266**, 26 (2019).
12. H. Remes, E. Korhonen, P. Lehto, *et al.*, J. Constr. Steel Res. **89**, 21 (2013).
13. W. Jinlong, M. Yuxin, P. Wenjie, *et al.*, Eng. Failure Anal. **153**, 107586 (2023).
14. R. Avilés, J. Albizuri, A. Lamikiz, *et al.*, Int. J. Fatigue **33**, 1477 (2011).
15. P. De Groot, Adv. Opt. Photonics **7**, 1 (2015).
16. Y. Zhou, Y. Tang, Y. Yang, *et al.*, Micromachines **8**, 319 (2017).
17. B. Bhaduri, C. Edwards, H. Pham, *et al.*, Adv. Opt. Photonics **6**, 57 (2014).
18. J. Sun, J. Wu, S. Wu, *et al.*, Light: Sci. Appl. **11**, 204 (2022).
19. L. Liu, E. Wang, X. Zhang, *et al.*, Sens. Actuators, A **215**, 89 (2014).
20. S. Fu, F. Cheng, T. Tjahjowidodo, *et al.*, Sensors **18**, 2657 (2018).
21. E. Gelenbe, T. Koçak, and R. Wang, Microelectron. Eng. **75**, 216 (2004).
22. K. Nakamae, Meas. Sci. Technol. **32**, 052003 (2021).
23. C. J. Tay, S. H. Wang, C. Quan, *et al.*, Opt. Laser Technol. **36**, 535 (2004).
24. F. Hui and M. Lanza, Nat. Electron. **2**, 221 (2019).
25. N. Kim, S. W. Lee, Y. I, *et al.*, Curr. Opt. Photon. **1**, 604 (2017).
26. K. Simonyan and A. Zisserman, in *International Conference on Learning Representations* (2015).
27. J. Kim, J. K. Lee, and K. M. Lee, in *2016 IEEE Conference on Computer Vision and Pattern Recognition (CVPR)* (2016), pp. 1646–1654.
28. N. Qian, Neural Netw. **12**, 145 (1999).

222.20.32.211 {ts '2024-08-12 21:25:48'}

Supplemental Document

Optics Letters

Deep-learning-assisted sidewall profiling white light interferometry system for accurately measuring 3D profiles and surface roughness on the groove sidewalls of precision components: supplement

XIANGYU ZHAO,[1] JINSONG ZHANG,[1] RENLONG ZHU,[2] YIJUN XIE,[2] ZHENGQIONG DONG,[2] LEI NIE,[2] SHIYUAN LIU,[1,3,5] AND JINLONG ZHU[1,3,4,*]

[1] *State Key Laboratory of Intelligent Manufacturing Equipment and Technology, Huazhong University of Science and Technology, Wuhan 430074, China*
[2] *Hubei Key Laboratory of Manufacture Quality Engineering, Hubei University of Technology, Wuhan 430068, China*
[3] *Optics Valley Laboratory, Wuhan, Hubei 430074, China*
[4] *Research Institute of Huazhong University of Science and Technology Shenzhen, Shenzhen 518057, China*
[5] *shyliu@hust.edu.cn*
[*] *jinlongzhu03@hust.edu.cn*

This supplement published with Optica Publishing Group on 12 August 2024 by The Authors under the terms of the Creative Commons Attribution 4.0 License in the format provided by the authors and unedited. Further distribution of this work must maintain attribution to the author(s) and the published article's title, journal citation, and DOI.

Supplement DOI: https://doi.org/10.6084/m9.figshare.26404411

Parent Article DOI: https://doi.org/10.1364/OL.531552

Deep-learning-assisted sidewall profiling white light interferometry system for accurately measuring 3D profiles and surface roughness on groove sidewalls of precision components: supplement

XIANGYU ZHAO,[1] JINSONG ZHANG,[1] RENLONG ZHU,[4] YIJUN XIE,[4] ZHENGQIONG DONG,[4] LEI NIE,[4] SHIYUAN LIU,[1,3,5] AND JINLONG ZHU [1,2,3,*]

[1] State Key Laboratory of Intelligent Manufacturing Equipment and Technology, Huazhong University of Science and Technology, Wuhan 430074, China
[2] Research Institute of Huazhong University of Science and Technology Shenzhen, Shenzhen 518057, China
[3] Optics Valley Laboratory, Wuhan, Hubei 430074, China
[4] Hubei Key Laboratory of Manufacture Quality Engineering, Hubei University of Technology, Wuhan, 430068, China
[5] shyliu@hust.edu.cn
**jinlongzhu03@hust.edu.cn*

Deep-learning-assisted sidewall profiling white light interferometry system for accurately measuring 3D profiles and surface roughness on groove sidewalls of precision components: supplemental document

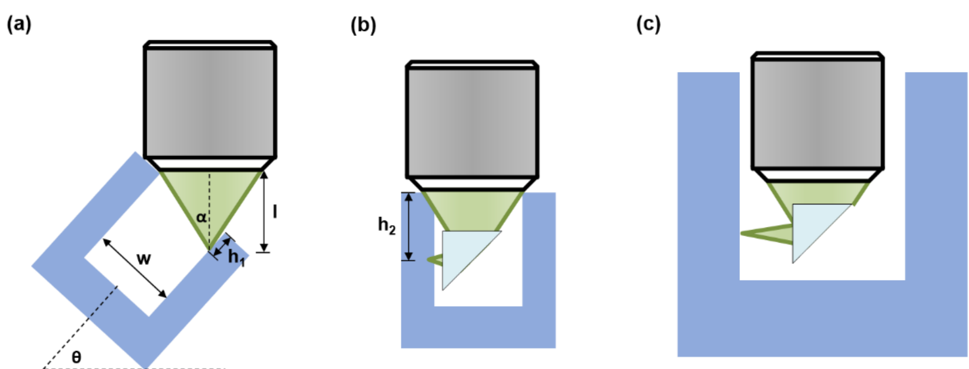

Fig. S1. Sidewall measurement for a small-diameter U-shaped sample using (a) the conventional WLI and (b) our proposed sidewall profiling white light interferometry (SPWLI) system. (c) Sidewall measurement for a large-diameter U-shaped sample using our proposed SPWLI system. Here w is the width of the groove, θ is the tilt angle of the sample, l is the working distance of the objective lens, α is half of the aperture angle of the objective, and h_1 is the maximum depth measured by the traditional WLI. h_2 is the maximum depth that can be measured by SPWLI.

To help better understand the advantage of SPWLI in terms of measuring grooves with large depth-to-width ratios, we use the following three schematics for better illustration: We take the measurement of the inner sidewall of a U-shaped sample as an example; as shown in Fig. S1. For a U-shaped sample with a small diameter, the groove sidewalls can be measured using a conventional WLI by tilting the sample (see the schematic in Fig. S1 (a)), whereas SPWLI can measure it vertically (see the schematic in Fig. S1 (b)). The ratio of the depth of the groove that can be measured by the conventional WLI to that by SPWLI h_1: h_2 is approximately $l \tan\alpha : l - m$, where l is the working distance of the objective lens, α is half of the aperture angle of the objective, and m is the edge length of the microprism, respectively. In the case of a measuring system using an objective lens with 0.15 NA and a working distance of 20 mm, h_1: h_2 is about 1:6, indicating that SPWLI could measure the depth-to-width ratio of grooves 6 times greater than conventional WLI. For a large-diameter U-shaped sample in which the entire objective can be inserted, the depth-to-width ratio can be infinite using SPWLI (see Fig. S1 (c)), which is not achievable using a conventional WLI.

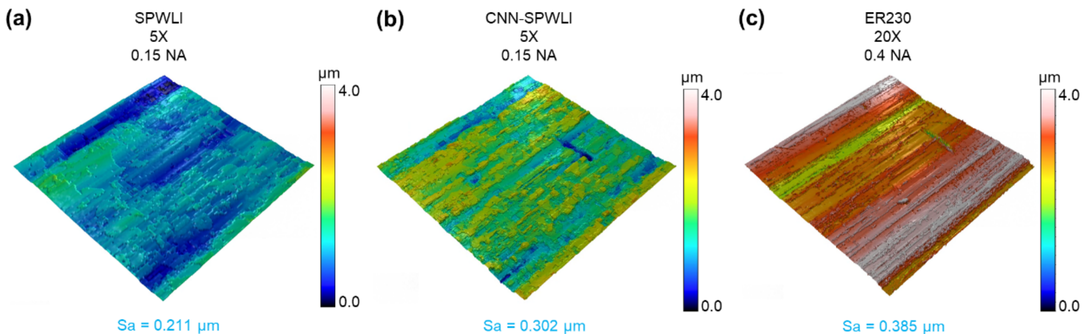

Fig. S2. The measurement results of surface roughness on the sidewall of a groove with a large depth-to-width ratio. The measurement results of surface roughness using (a) the SPWLI with a 0.15-NA objective, (b) the CNN-SPWLI with a 0.15-NA objective, and (c) the ER230 with a 0.4-NA objective, respectively. The measurement areas are 200 μm wide by 200 μm long.

The SPWLI, CNN-SPWLI, and the commercial WLI (ER230) were used to respectively measure the surface roughness on the sidewall of a machined component with a 80-mm wide and 200-mm deep groove. The surface roughness on the groove sidewall of the component was firstly measured by the SPWLI with a 0.15-NA objective, after which the CNN-based SISR processing was applied to enhance the measurement results from SPWLI. We cut the component along the edge of the groove, after which the commercial ER230 WLI (equipped with a 0.4-NA objective) was utilized to measure the same surface area. As a result, the measured value by ER230 is treated as the golden standard for the comparison. As shown in Fig. S2, the measured Sa for area of interest on the sidewall using CNN-SPWLI is 0.302 μm (Fig. S2(b)), which is closer to the golden standard (see Fig. S2(c)) when compared to the ones measured by SPWLI (see Fig. S2(a)). In conclusion, the Sa reconstructed by CNN-SPWLI is improved by 52.30%.